International Journal of Pharmacy and Pharmaceutical Sciences

ISSN- 0975-1491 Vol 8, Issue 2, 2016

Original Article

TRANSCRIPTOME-WIDE ANALYSIS OF NFX1 TRANSCRIPTION FACTORS IN WHEAT (*TRITICUM AESTIVUM* L.) AND THEIR LEAF RUST RESPONSIVE EXPRESSION PROFILING

LOPAMUDRA SATAPATHY, KUNAL MUKHOPADHYAY

Department of Bio-Engineering, Birla Institute of Technology, Mesra, Ranchi 835215, India
Email: kmukhopadhyay@bitmesra.ac.in

Received: 18 Nov 2015 Revised and Accepted: 12 Dec 2015

ABSTRACT

Objective: The purpose of this study was to identify and characterize NFX1 transcription factors (TFs) in wheat and study their expression profiles in response to leaf rust infection.

Methods: NFX1 transcription factors were identified by *in silico* data-mining, followed by characterisation using different bioinformatics tool. The evolutionary relationship was established by constructing a phylogenetic tree with *Arabidopsis* NFX1 proteins using Molecular Evolutionary Genetic Analysis (MEGA5). Expression analysis of identified TaNFX1 TFs in wheat was performed using CLC Genomics Workbench.

Results: Nine NFX1 transcription factors were identified in wheat. Evolutionary analysis revealed their classification into group 1, 2 and 4 type NFX1 zinc finger. Tag based expression analysis revealed that based on the fold change values, the maximum level of expression was observed in *TaNFX1-3* and *7* whereas, the minimum level of expression was observed in *TaNFX1-2* in response to leaf rust pathogenesis. Chromosomal localization predicted that identified NFX1 sequences belonged to 3A, 3B, 3D and 7D chromosomes.

Conclusion: Using transcriptomic approach nine NFX1 TF proteins are predicted that regulate gene expression in response to leaf rust disease in wheat which has not been reported or studied before. Functional and bioinformatics-based exploration of wheat NFX1 TFs in related monocots might provide subsets of candidate target genes to improve agronomic traits related to biotic stress tolerance.

Keywords: Wheat, Biotic stress, NFX1, RING finger

INTRODUCTION

Wheat (*Triticum aestivum* L.) is a member of the Poaceae family and provides 40-60% of calories in human diets. It is one of the vital sources of food for a large part of the world's population covering 18.8% of daily caloric intake in human diet [1]. The demand of wheat is expected to increase by 60% by the year 2050, whereas the production is estimated to decrease 29% due to environmental stress factors including both biotic and abiotic stress [2]. Hence, comprehension of molecular mechanisms such as transcription factors (TFs) underlying the stress tolerance in wheat has a great importance for improvement of wheat cultivars [3].

NFX1 proteins present in eukaryotes represent a class of TFs which are characterized by NFX1-type zinc finger motifs. Currently, 176 NFX1 TFs have been identified in plants and submitted to Plant Transcription Factor Database (PTFDB), Peking University (http://planttfdb. cbi. pku. edu. cn/). In *Arabidopsis*, two NFX1 homologs, AtNFXL1 and AtNFXL2 have been identified which are characterized by NFX1 type zinc fingers and PHD finger motifs. NFX1 type zinc finger motifs mediate DNA binding and PHD finger motifs located in nuclear proteins is involved in chromatin-mediated transcriptional regulation and also mediates protein interactions [4]. The AtNFXL1 protein is a part of regulatory mechanism, which improves the physiological status of plants and supports growth and survival under stress [5]. Besides these two domains, a RING finger domain is located within the N-terminus [6]. RING finger proteins are found in both nucleus and cytoplasm [7]. They function as ubiquitin ligases that interact with specific substrates and combination with ubiquitin-conjugating enzymes (E2s) confer ubiquitination to target proteins *in vitro* and *in vivo*. In wheat, four NFX1 protein sequences are available at PTFDB. Plant NFX1-like proteins modulate growth and survival by coordinating Reactive Oxygen Species (ROS), Salicylic Acid (SA), biotic stress and Abscisic Acid (ABA) responses. These plant proteins possessed both specific C4HC3 RING finger motif and conserved Cys-rich region including NFX1-type zinc finger motifs as present in human NFX1 protein. PHD finger consists of a C4HC3 Zn-ligand signature. In case of RING finger domains, different arrangements such as C3H2C3 (RING-H2) [8], or C3HC4 (RINGHC) [9], also C4HC3 (RING-CH) [10], C2H2C4 [11] and C8 [12] are known. Leaf (brown) rust disease in wheat caused by obligate biotrophic fungus *Puccinia triticina* Eriks. is one of the most common rust disease occurring world wide than stem rust (*P. graminis f.* sp. *tritici*) or stripe rust (*P. striiformis f.* sp. *tritici*) of wheat. The present study was undertaken with the aim to identify, characterize NFX1 TFs in wheat and to decipher their roles during leaf rust pathogenesis.

MATERIALS AND METHODS

In silico data mining of NFX1 TFs and phylogenetic analysis

All available NFX1 nucleotide and protein sequences were retrieved from different species (*Brachypodium distachyon*, *Oryza sativa* subsp. *Indica*, *Oryza sativa* subsp. *japonica*, *Sorghum bicolor*, *Triticum uratu* and *Zea mays*) from PTFDB. The retrieved nucleotide sequences were searched for similarity with wheat Expressed Sequence Tags (ESTs) using Basic Local Alignment Search Tool (BLAST) at National Centre for Biotechnology (NCBI) with an e-value cut-off of 10 [13-15]. The no redundant ESTs were selected, translated *in silico* using GENSCAN and only the sequences containing conserved NFX1 domains opted for further characterization. BLASTN was performed with their respective nucleic acid sequences in order to check for novelty. Phylogenetic analysis of newly identified NFX1 proteins in wheat was performed to study their evolutionary relationship with known *Arabidopsis* sequences based on Multiple Sequence Alignments (MSA) and Un weighed Pair Group Method with Arithmetic Mean (UPGMA) method using Molecular Evolutionary Genetic Analysis MEGA5 software [16]. Bootstrap analysis of 1000 replicates was carried out to provide confidence estimates for the tree topology.

In silico characterization of identified NF-X1 TFs in wheat

The theoretical pI and molecular weight[17] was determined for the identified TaNFX1 TFs using ExPASy Server (http://us. expasy. org/tools/pi_tool. html), whereas, the number of positively and

negatively charged amino acid residues, atomic composition, the grand average of hydropathicity (GRAVY) and the aliphatic index was analyzed using Prot Param [18]. Kinase-specific phosphorylation sites [19] and N-glycosylation potential sites [20] were predicted for the identified TaNFX1 TFs by NetPhos 2.0 Server (http://www. cbs. dtu. dk) and NetNGlyc 1.0 Server (http://www. cbs. dtu. dk) respectively. Transmembrane helices and nuclear localization signals (NLS) present in the newly identified sequences were predicted using HMMTOP [21] and NLStradamus [22] software respectively. A cut-off value of 0.6 and Viterbi algorithm was used to determine the position and their corresponding amino acid sequences of the NLS. Secondary structures were predicted for the identified NFX1 proteins using CLC genomics workbench 6.5. A functional interacting network of proteins was performed using STRING 10 software [23] with a confidence value of 0.15.

Chromosomal localization

Chromosomal localization of the identified NFX1 TFs in wheat was performed using URGI portal using the BLAST tool (http://wheat-urgi. versailles. inra. fr/Seq-Repository/BLAST) with a e-value of 0.0001.

RNA isolation, serial analysis of gene expression (SAGE) library preparation and next generation sequencing

A pair of wheat Near Isogenic Lines (NILs): HD2329 (seedling leaf rust susceptible phenotype, infection type 3+) and HD2329+*Lr28* (seedling leaf rust resistant; Nest Immune infection type 0-0) were used in the study. *Puccinia triticina* pathotype 77-5, the most predominant and devastating leaf rust pathogen in all parts of the Indian subcontinent, was selected as the experimental pathogen [24]. The pathogen inoculum was prepared by mixing urediniospores of *P. triticina* pathotype 77-5 and talcum powder (ratio 1:1) and applied gently on moist leaves of the NIL pairs. Both plant types were also mock inoculated with only talcum powder and used as a control. Plants were placed under a high humidity of >90% for 24 h post inoculation (hpi) in the dark to facilitate infection. Then the pots were transferred to the normal growth chamber (22 °C daytime; 14 °C night time; relative humidity-80%) at the National Phytotron Facility, Indian Agriculture Research Institute, New Delhi. Leaf tissues from 15 seedlings in each treatment were collected at 24 hpi and stored in liquid nitrogen. Total RNA isolation from leaf samples using TRI REAGENT (Molecular Research Centre, Inc., USA) was carried out as per manufacturer's instruction [25].

The integrity of the isolated RNAs was confirmed using Agilent Bio analyser 2100. Four SAGE libraries were prepared from the isolated RNAs [coded as: (i) Susceptible-Mock (S-M): HD2329 mock inoculated, (ii) Susceptible-Pathogen Inoculated (S-PI): HD2329 pathogen-inoculated, (iii) Resistant Mock (R-M): HD2329+*Lr*28 mock inoculated and (iv) Resistant-Pathogen Inoculated (R-PI): HD2329+*Lr*28 pathogen inoculated] using SOLiD (Sequencing by Oligonucleotide Ligation and Detection) SAGE kit (Applied Biosystems, CA, USA) following the recommended protocol and sequenced using SOLiD technique at Bay Zoltán Foundation of Applied Research, Institute of Plant Genomics, Human Biotechnology and Bioenergy, Zagreb, Hungary. The sequences have been submitted to NCBI SRA061917 (Bio Sample accession as SAMM01820702, SAMM01820703, SAMM01820704 and SAMM01820705).

Expression analysis of identified TaNFX1 TFs in wheat under biotic stress

Expression values for all the identified TaNFX1 TFs in wheat were extracted from the four SOLiD-SAGE datasets using CLC Genomics Workbench 6.5. The differential expression of the identified TaNFX1 transcripts among the wheat NILs in response to leaf rust pathogenesis was determined with log2 transformed values and represented through heat map scatter plot and volcano plots.

RESULTS

***In silico* identification of NFX1 TFs in wheat and phylogenetic analysis**

Two nucleotide sequences of *Arabidopsis thaliana*, one from *B. distachyon*, five from *O. sativa indica*, four from *O. sativa japonica*, three from *S. bicolor*, two from *T. uratu* and one sequence from *Z. mays* could be retrieved from PTFDB. After blastn with wheat ESTs and removal of redundant sequences, nine sequences were identified in wheat (table 1). Previously four wheat NFX1 sequences were submitted PTFDB making the total number of NFX1 sequences to 13 in wheat.

The evolutionary analysis was performed for the nine newly identified NFX1 TFs in wheat with respect to NFX1 protein sequences of *Arabidopsis thaliana* (fig.1). Phylogenetic tree was classified into two clades. It was found that TaNFX1-1, 2, 6 and 9 belonged to Group 1 NFX1 type zinc finger. TaNFX1-4, 5 and At NFX1-2 belonged to Group 2 NFX1 type zinc finger. TaNFX1-3, 7, 8 and AtNFX1-1 belonged to Group 4 NFX1 type zinc finger.

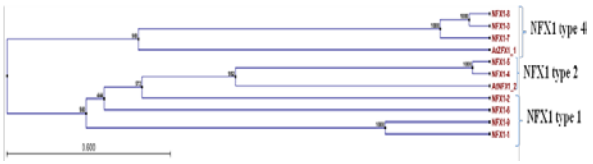

Fig. 1: Phylogenetic tree of TaNFX1 proteins with known *Arabidopsis* sequences. Source: author's own results

***In silico* characterization of novel wheat NFX1 protein**

The phosphorylation-site analysis provides definitive information on functional relationships between signaling proteins. N-phosphorylation occurs in serine, threonine and tyrosine residue which affects a multitude of cellular signaling processes. Any potential crossing the threshold of 0.5 represented a predicted phosphorylated site. Serine and threonine phosphorylation sites were found in all the identified NFX1 proteins. Tryptophan sites were absent in NFX1-2, 3, 7 and 8 proteins (table 1). Glycosylation plays a critical role in determining protein structure, function and stability. Structurally, glycosylation is deemed to affect the three-dimensional configuration of proteins.

Table 1: Prediction of atomic composition, glycosylation and phosphorylation sites in wheat NFX1 TF proteins

S. No.	NFX1 protein identified	EST sequence Accession Number at NCBI	Atomic composition					Glycosylation sites with threshold 0.5	Kinase-specific phosphorylation sites with threshold 0.5		
			C	H	N	O	S		Serine	Threonine	Tryptophan
1	NFX1-1	CJ835435	912	1491	277	252	17	-	1	1	3
2	NFX1-2	HX191466	914	1419	281	265	30	-	7	1	0
3	NFX1-3	CJ720243	852	1374	278	267	30	-	7	2	0
4	NFX1-4	HX191494	1105	1838	376	320	49	-	2	3	1
5	NFX1-5	CJ592487	1056	1757	363	304	48	-	1	1	1
6	NFX1-6	CA729903	872	1397	261	257	28	1	4	3	3
7	NFX1-7	BJ267736	905	1463	287	283	24	-	7	2	0
8	NFX1-8	HX143764	958	1532	302	289	30	-	5	2	0
9	NFX1-9	CV780566	495	778	152	137	13	-	3	1	2

Source: author's own design

Therefore, glycosylation plays a vital role in determining the cellular response to exogenous factors. N-glycosylation occurs in asparagine amino acid residue present in Asn/Xaa-Ser/Thr stretches where Xaa can be any amino acid except proline. This consensus tripeptide is referred to as N-glycosylation sequon. Any potential crossing the threshold of 0.5 represented a predicted glycosylated site. Glycosylation specific prediction sites were found in NFX1-6 protein only (table 1).

Using Protparam, instability index of TaNFX1 proteins was predicted, and all proteins were found to be unstable (table 2). The aliphatic index is an indication for the increase in thermostability of globular proteins. High aliphatic index indicates thermal stability and flexible nature of proteins. The highest aliphatic value was found in NFX1-1 protein, and the lowest value was found in NFX1-5 protein (table 2). GRAVY values normally range between±2 where positive values are indicators of hydrophobic nature of proteins, and negative values indicate hydrophilic nature of proteins. All the identified NFX1 proteins were considered to be hydrophilic in nature (table 2). Transmembrane helices play a vital role in the study of membrane-associated proteins especially with respect to cell signaling, energy transduction, and transport. Two such helices were found only in NFX1-1 protein at positions 90-107 and 167-178. In rest of NFX1 proteins, transmembrane helices were absent. NLS was identified in NFX1-1 protein only. The secondary structure could be predicted for all the nine NFX1 proteins. Beta strands were present in all the NFX1 proteins whereas alpha helix was absent in NFX1-3 (table 3).

Direct and indirect functional associations of the predicted NFX1 (fig. 2) proteins in wheat were established using STRING 10 software. Colored nodes indicated their direct association with the input whereas, the edges predicted functional links i.e. they consisted of up to eight lines: one color for each type of evidence. TaNFX1 network formed is a hub-based network involving multifunctional proteins denoted as hubs. It was linked with *Arabidopsis* NFX1 proteins which were involved in biological processes, a molecular function such as binding activity.

Chromosomal localization

TaNFX1-2, 4, 5 and 9 were found to be localized in wheat chromosome 3B whereas, TaNFX1-1 was found to be localized in the short arm of wheat chromosome 3D. TaNFX1-3, 7 and 8 were localized in the long arm of wheat chromosome 7D. TaNFX1-6 was localized in the short arm of wheat chromosome 3A (table 3).

SOLiD-SAGE based expression analysis of identified NFX1 TFs in wheat under leaf rust pathogenesis

In order to identify the differentially expressed *TaNFX1* genes in response to leaf rust pathogenesis, the identified *NFX1* genes were mapped to the reads from the four SOLiD-SAGE libraries using CLC Genomics Workbench 6.5 (supplementary file 1).

In order to identify the expression of a represented gene for a given tag, the tags are often compared to a virtual library of tags that would have been extracted from an annotated genome or a set of ESTs (supplementary file 2). Pair wise experiments were conducted between libraries using differentially expressed reads of TaNFX1 with log2 transformed values to obtain feature hierarchical clustering and were displayed as a heat map (fig. 3). A total of differentially expressed 34 tags could be extracted from four libraries and their corresponding *TaNFX1* genes were determined (supplementary file 3). Based on the fold change values, the maximum level of expression was observed in *TaNFX1-3* and *7*; the minimum level of expression was observed in *TaNFX1-2*. It was noted that many *TaNFX1* genes such as *TaNFX1-3, 4, 5, 7* and *8* represented the same tag. This might be due to the presence of conserved region between the two genes [15].

Tag counts for *TaNFX1*genes in S-M, S-PI, R-M and R-PI libraries were found to be 4734, 6650, 1967, and 2203 respectively. Quantitative comparison of the differentially expressed *TaNFX1* genes during infection of wheat NILs was performed using two-dimensional scatter plots showing Pearson correlation coefficients between the SAGE libraries (fig. 4a, 4b and 4c). Pearson correlation coefficients were 0.34, 0.55 and 0.25 for S-M vs. S-PI, R-M vs. R-PI and S-PI vs. R-PI libraries respectively in TaNFX1 (fig.4a, 4b and 4c). Volcano plot, another type of scatter plot, was constructed by plotting the negative log of the p-value on the y-axis (usually base 10) where the x-axis is the log of the fold changes between the two conditions that changes in both directions (up and down) and appear equidistant from the center (fig. 5a, 5b and 5c; supplementary file 4). Data points with low p-values, indicating high significance, appeared towards the top of the plot. Experiments between S-M vs. S-PI showed, *TaNFX1-3*, *6* and *7* to have the lowest p-value and appeared towards the top of the plot (fig. 5a). *TaNFX1-1*, *4*, *5*, *6* and *9* had low p-values and were hence present towards the top of the plot in the experiment R-M vs. R-PI (fig. 5b). *TaNFX1-4*, *6* and *9* had the lowest p-value and were, therefore, present at the top of the plot in the experiment between S-PI vs. R-PI (fig. 5c).

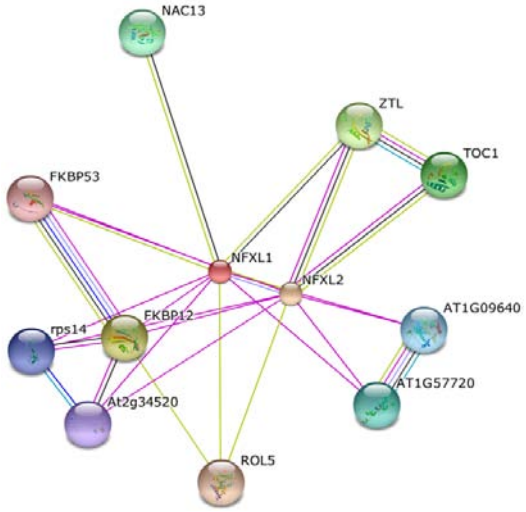

Fig. 2: Protein–protein interactions of wheat NFX1 proteins using STRING. Source: author's own results

Table 2: *In-silico* characterisation of NFX1 TF proteins in wheat

S. No.	NFX1 TF	No. of amino acids	Molecular weight (Da)	Theoretical pI	Total no. of atoms	Extinction coefficient	Total negative residues	Total positive residues	Instability Index	Aliphatic index	GRAVY value
1	NFX1-1	186	20913.6	9.52	2949	24700	14	31	45.59	82.69	-0.382
2	NFX1-2	196	21545.8	8.21	2909	28220	16	21	57.47	53.78	-0.365
3	NFX1-3	197	20745.7	8.25	2801	3115	15	20	62.05	50.46	-0.420
4	NFX1-4	241	27082.0	8.99	3688	7345	24	50	65.8	46.1	-0.660
5	NFX1-5	232	25941.7	9.02	3528	7345	22	49	66.59	44.14	-0.691
6	NFX1-6	184	20546.9	8.27	2815	5970	18	23	54.93	63.04	-0.440
7	NFX1-7	201	21667.7	8.24	2962	6990	20	24	61.54	61.99	-0.448
8	NFX1-8	214	22866.3	8.14	3111	8490	18	22	66.63	58.32	-0.323
9	NFX1-9	99	11467.3	9.34	1575	27095	6	16	77.27	52.12	-0.726

Source: author's own design

Table 3: Prediction of transmembrane helices, secondary structures and chromosomal localisation of NFX1 TFs in wheat

S. No.	NFX1 TF	Transmembrane helices position	Nuclear localization signals	Secondary structure prediction		Chromosome localization
				Alpha helix	Beta strand	
1	NFX1-1	90-107, 161-178	132-TNVPKRRKKRDR-143	5-21, 51-55, 69-81, 113-122, 154-156	5-10, 42, 58, 60-62, 96-100, 108-109, 130-131, 150-152, 159-184	3DS
2	NFX1-2	-	-	182-189, 191-193	14-15, 21-24, 51-53, 63-66, 79, 103-107, 119, 125-126, 151	3B
3	NFX1-3	-	-	-	23-30, 34-38, 47-48, 90-91, 95, 121, 125-130, 134-139, 154-158, 181-182	7DL
4	NFX1-4	-	-	3-5, 8-14, 121-129, 212-214	63, 75, 93-100, 130-140, 179-183, 187-191, 235-236	3B
5	NFX1-5	-	-	102-110, 193-195	54-56, 74-81, 119-121, 160-164, 168-172, 216-217	3B
6	NFX1-6	-	-	34-40, 114-117	41, 54-59, 88-89, 95, 101-104, 160-164, 174-181	3AS
7	NFX1-7	-	-	151-166, 173-177, 184-193	12-13, 55-56, 86, 90-95, 99-104, 120-123, 147	7DL
8	NFX1-8	-	-	186-201, 208-212	23-31, 33-38, 47-48, 90-91, 95, 121, 125-130, 134-139, 154-158, 181-182	7DL
9	NFX1-9	-	-	15-21, 69-84	5-9, 42, 58, 60-62	3B

Source: author's own design

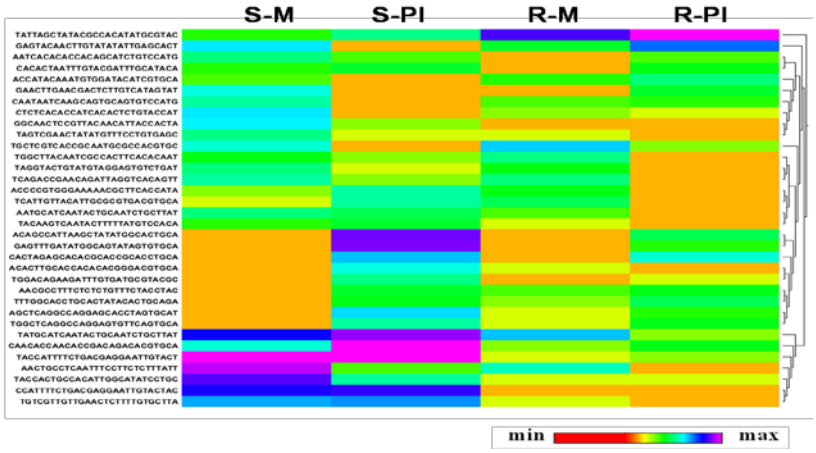

Fig. 3: Heat map of identified *NFX1* genes in wheat. Source: author's own results

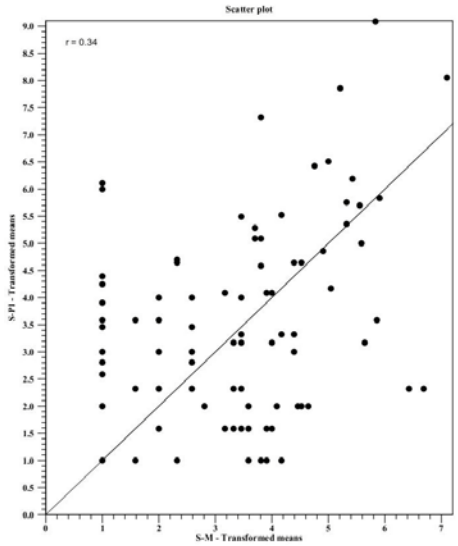

Fig. 4a: Scatter plot of identified *NFX1* genes in wheat in S-M vs S-PI libraries. Source: author's own results

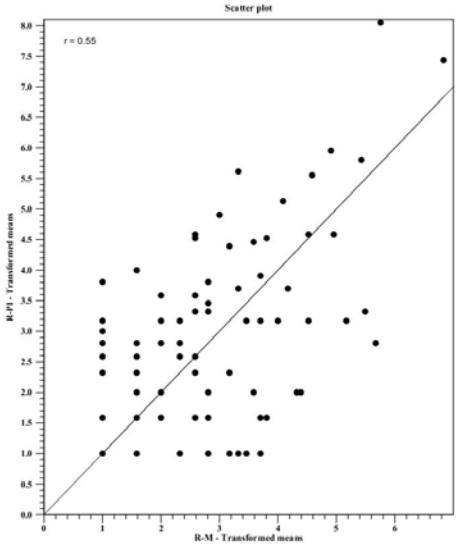

Fig. 4b: Scatter plot of identified *NFX1* genes in wheat in R-M vs R-PI libraries. Source: author's own results

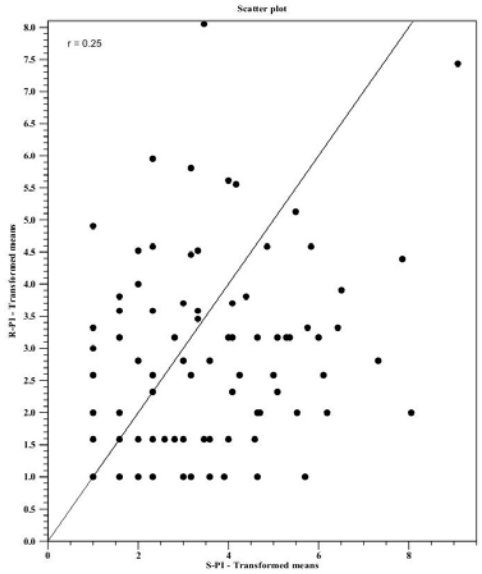

Fig. 4c: Scatter plot of identified *NFX1* genes in wheat in S-PI vs R-PI libraries. Source: author's own results

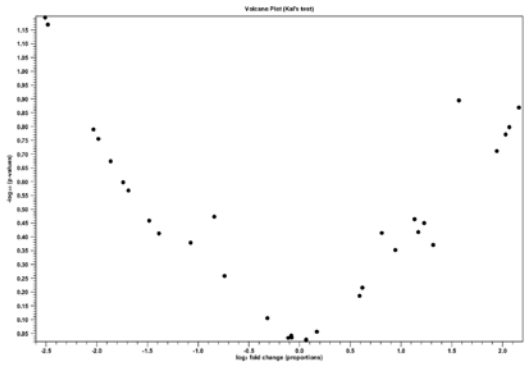

Fig. 5a: Volcano plot of NFX1 TF in S-M vs S-PI libraries. Source: author's own results

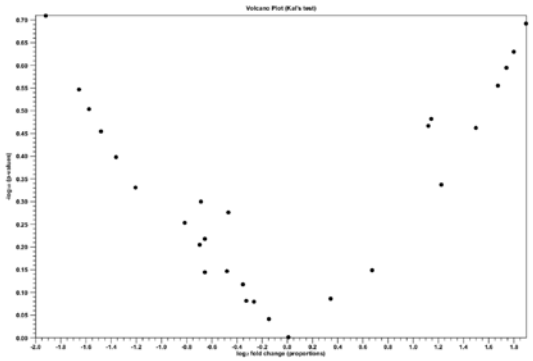

Fig. 5b: Volcano plot of NFX1 TF in R-M vs R-PI libraries. Source: author's own results

DISCUSSION

NFX1 type TFs have been identified characterized, and their roles in stress have been deciphered in *Arabidopsis thaliana.* No reports on wheat NFX1 TF are available yet. This is the first report on wheat NFX1 TFs where they have been identified, characterized and their role in leaf rust pathogenesis has been predicted. The instability index is an estimate of the protein stability under *in vitro* conditions. Protein with instability index less than 40 is predicted as stable, and a value above 40 predicts the unstable nature of the protein, hence all identified NF-X1 proteins was unstable by nature. Protein-protein interactions of NFX1 proteins showed that they are linked with *Arabidopsis* NFX1 proteins which have a role to play in biotic and abiotic stress. Besides, these proteins have a role in plant circadian rhythm pathway as predicted by KEGG pathway analysis.

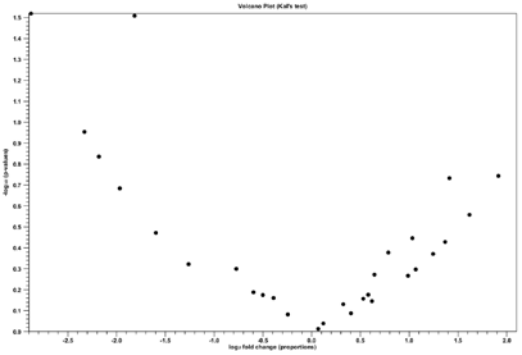

Fig. 5c: Volcano plot of NFX1 TF in S-PI vs R-PI libraries. Source: author's own results

The phylogenetic tree showed that identified NFX1 proteins belonged to type-1, 2 and 4 NFX1zinc finger. Tag-based transcriptomics analysis is an extension of SAGE in conjunction with next-generation sequencing technologies, where the full-length mRNAs are not sequenced. Tags of 27 bp are extracted from each transcript, sequenced and counted to measure the abundance of each transcript. Among all the three experiments performed for scatter plot, the highest differences in expression of *TaNFX1*genes between two libraries were in R-M vs. R-PI. This suggests that the wheat NILs employ different sets of *TaNFX1* genes to counter leaf rust pathogen-mediated infection.

CONCLUSION

In this study using the transcriptomic approach we have predicted NFX1 TF proteins that regulate gene expression in response to leaf rust disease in wheat which has not been reported or studied before. We were able to get differentially expressed *NFX1* genes indicating their role in leaf rust pathogenesis. Functional and bioinformatics-based exploration of wheat NFX1 TFs in related monocots might provide subsets of candidate target genes to improve agronomic traits related to biotic stress tolerance.

Availability

Sequence read archives: SRA061917 under Bio Sample accessions for four SOLiD SAGE libraries: SAMN01820702, SAMN01820703, SAMN01820704, and SAMN01820705.

ACKNOWLEDGEMENT

This work was supported by Department of Biotechnology, Government of India (Grant No. BT/PR6037/AGR/02/308/05), BTISNet SubDIC (BT/BI/04/065/04), Department of Agriculture, Government of Jharkhand (5/B. K. V/Misc/12/2001) and CoE-TEQIP-II (Grant No. NPIU/TEQIP II/FIN/31/158). L. S. is grateful to Department of Science and Technology-INSPIRE (Fellowship/ 2011/318) for PhD. fellowship. The authors acknowledge Dr. KV Prabhu for providing Phytotron facility and carrying infectivity studies at IARI, New Delhi, India and Dr. D. Singh for the preparation of SOLiD-SAGE libraries.

CONFLICT OF INTERESTS

Declared none

REFERENCES

1. FAO. Food and agriculture organization of the United Nations. Available from http://www.fao.org. [Last accessed on 10 Feb 2015].

2. Manickavelu A, Kawaura K, Oishi K, Shin IT, Kohara Y, Yahiaoui N, *et al.* Comprehensive functional analyses of expressed sequence tags in common wheat (*Triticum aestivum*). DNA Res 2012;19:165–77.
3. Okay S, Derelli E, Unver T. Transcriptome-wide identification of bread wheat WRKY transcription factors in response to drought stress. Mol Genet Genomics 2014;289:765-81.
4. Aasland R, Gibson TJ, Stewart AF. The PHD finger: implications for chromatin-mediated transcriptional regulation. Trends Biochem Sci 1995;20:56–9.
5. Lisso J, Altmann T, Mussig C. The AtNFXL1 gene encodes a NFX1 type zinc finger protein required for growth under salt stress. FEBS Lett 2006;580:4851-6.
6. Mussig C, Schroder F, Usadel P, Lisso J. Structure and putative function of NFX1-like proteins in plants. Plant Biol 2009;12:381-94.
7. Borden KLB. RING domains: master builders of molecular scaffolds. J Mol Biol 2000;295:1103–12.
8. Katoh S, Hong C, Tsunoda Y, Murata K, Takai R, Minami E, *et al.* High-precision NMR structure and function of the RING-H2 finger domain of EL5, a rice protein whose expression is increased upon exposure to pathogen derived oligosaccharides. J Biol Chem 2003;278:15341–8.
9. Mercier P, Lewis MJ, Hau DD, Saltibus LF, Xiao W, Spyracopoulos L. Structure, interactions, and dynamics of the RING domain from human TRAF6. Protein Sci 2007;16:602–14.
10. Dodd RB, Allen MD, Brown SE, Sanderson CM, Duncan LM, Lehner PJ, *et al.* Solution structure of the kaposi's sarcoma-associated herpesvirus K3 N-terminal domain reveals a novel E2-binding C3HC4-type RING domain. J Biol Chem 2004:279:53840–7.
11. Kostic M, Matt T, Martinez-Yamouta MA, Dysona HJ, Wright PE. Solution structure of the Hdm2 C2H2C4 RING, a domain critical for ubiquitination of p53. J Mol Biol 2006;363:433–50.
12. Kellenberger E, Dominguez C, Fribourg S, Wasielewski E, Moras D, Poterszman A, *et al.* Solution structure of the C-terminal domain of TFIIH P44 subunit reveals a novel type of C4C4 ring domain involved in protein–protein interactions. J Biol Chem 2005;280:20785–92.
13. Niu C, Wei W, Zhou Q, Tian A, Hao Y, Zhang W, *et al.* Wheat *WRKY* genes *TaWRKY2 and TaWRKY19* regulate abiotic stress tolerance in transgenic *Arabidopsis* plants. Plant Cell Environ 2012;35:1156-70.
14. Xiaoming S, Gaofeng L, Weike D, Tongkun L, Zhinan H, Jun R, *et al.* Genome-wide identification, classification and expression analysis of the heat shock transcription factor family in Chinese cabbage. Mol Genet Genomics 2014;289:541-51.
15. Satapathy L, Singh D, Ranjan P, Kumar D, Kumar M, Prabhu KV, *et al.* Transcriptome-wide analysis of WRKY transcription factors in wheat and their leaf rust responsive expression profiling. Mol Genet Genomics 2014;289:1289-306.
16. Tamura K, Peterson D, Stecher G, Nei M, Kumar S. MEGA5: molecular evolutionary genetics analysis using maximum likelihood, evolutionary distance, and maximum parsimony methods. Mol Biol Evol 2011;28:2731-9.
17. Bjellqvist B, Basse B, Olsen E, Celis JE. Reference points for comparisons of two-dimensional maps of proteins from different human cell types defined in a pH scale where isoelectric points correlate with polypeptide compositions. Electrophoresis 1994;15:529-39.
18. Gasteiger E, Hoogland C, Gattiker A, Duvaud S, Wilkins MR, Appel RD, *et al.* Protein identification and analysis tools on the ExPASy server. The proteomics protocols handbook, Humana Press; 2005.
19. Blom N, Gammeltoft S, Brunak S. Sequence and structure-based prediction of eukaryotic protein phosphorylation sites. J Mol Biol 1999;294:1351-62.
20. Gupta R, Jung E, Brunak S. Prediction of N-glycosylation sites in human proteins. Pac Symp Biocomput 2004;7:310-22.
21. Garg B, Puranik S, Misra S, Tripathy BN, Prasad M. Transcript profiling identifies novel transcripts with unknown functions as primary response components to osmotic stress in wheat (*Triticum aestivum* L.). Plant Cell Tissue Organ Cult 2013;113:91-101.
22. Nguyen BAN, Pogoutse A, Provart N, Moses AM. NL Stradamus: a simple hidden markov model for nuclear localization signal prediction. BMC Bioinf 2009;10:202.
23. Franceschini A, Szklarczyk D, Frankild S, Kuhn M, Simonovic M, Roth A, *et al.* STRING v9.1: protein-protein interaction networks, with increased coverage and integration. Nucleic Acids Res 2013;41:808-15.
24. Bipinraj A, Honrao B, Prashar M, Bhardwaj S, Rao S, Tamhankar S. Validation and identification of molecular markers linked to the leaf rust resistance gene *Lr28* in wheat. J Appl Genet 2011;52:171-5.
25. Singh D, Bhaganagare G, Bandopadhyay R, Prabhu KV, Gupta PK, Mukhopadhyay K. Targeted spatiotemporal expression based characterization of the state of infection and time-point of maximum defense in wheat NILs during leaf rust infection. Mol Biol Rep 2012;39:9373-82.